IEEE Access
Multidisciplinary ⋮ Rapid Review ⋮ Open Access Journal

Received 19 July 2024, accepted 9 August 2024, date of publication 19 August 2024, date of current version 29 August 2024.

Digital Object Identifier 10.1109/ACCESS.2024.3445955

RESEARCH ARTICLE

Integrating Level Shift Anomaly Detection for Fault Diagnosis of Battery Management System for Lithium-Ion Batteries

DASARI HETHU AVINASH[1] **AND A. RAMMOHAN**[2]
[1]School of Electrical Engineering, Vellore Institute of Technology (VIT), Vellore 632014, India
[2]Automotive Research Center, VIT, Vellore 632014, India

Corresponding author: A. Rammohan (rammohan.a@vit.ac.in)

This work was supported by the Office of the Dean, Academic Research Vellore Institute of Technology (VIT), Vellore.

ABSTRACT This study analyzes the mechanism of Internal Short Circuits (ISCs) in Lithium-ion batteries (LIBs) and identifies the factors contributing to their development. A simulation environment has been used to design a custom battery pack with a nominal capacity of $3kWh$(total pack capacity 62.5 Ah) and conduct various fault simulations to analyze the battery pack's thermal behaviour under different conditions. The discharge rate is variable, with a value of $0.25C$ for all 18650 LIBs, and the temperature ranges from -20°C to +60°C. The collected temperature data has been preprocessed and analyzed using various anomaly detection algorithms, including the proposed LevelshiftAD method, Isolation Forest, and Elliptical Envelope. The study demonstrates that the proposed LevelshiftAD method performs better in accurately detecting temperature faults at the threshold limit faster than the other anomaly detection methods. These findings highlight the potential of the proposed approach for enhancing the accuracy with 97% and efficacy of fault diagnosis in LIBs.

INDEX TERMS Anomaly detection, battery management system, elliptical envelop, isolation forest, lithium-ion batteries, level shift anomaly detection method.

ABBREVIATIONS AND ACRONYMS

AD -	Anomaly Detection.
BMS -	Battery Management System.
EV -	Electric Vehicle.
EKF -	Extended Kalman Filter.
EE -	Elliptical Envelop.
IF -	Isolation Forest.
ISC -	Internal Short-Circuit.
IQR-	Interquartile range.
LIB -	Lithium-ion Battery.
MCU -	Micro Controller Unit.
MCA-	Minimum Covariance Determinant.
ML -	Machine Learning.
RF-	Random Forest.

The associate editor coordinating the review of this manuscript and approving it for publication was Vitor Monteiro.

I. INTRODUCTION

Electric vehicles (EVs) are revolutionizing the transportation industry by promoting sustainable mobility. The success of EVs largely depends on the selection and use of advanced energy storage systems [1], such as rechargeable batteries. These batteries are available in different types, including lead-acid, nickel-sodium, and lithium-ion, each with unique properties. Among these types, lithium-ion batteries (LIBs) are the most popular choice for EVs due to their high energy density, long lifespan, and efficiency. However, as the primary energy source for EVs, LIBs are exposed to various operational stresses and environmental factors that can lead to degradation and potential faults [2]. Research in EV and energy storage industries plays an essential role in developing and implementing battery management systems (BMS) in EVs. This research focuses on enhancing battery performance, extending battery life, and ensuring the safe and efficient operation of EV batteries. Concerns about energy

security, environmental impacts, and innovations within the automotive industry drive the rapid progress of EVs. The LIBs have become the leading power source for EVs because of their high energy and power density, as well as their long service life. However, ensuring their safety remains a significant challenge, with internal short circuits being a primary cause of lithium-ion battery failures, potentially leading to serious safety incidents such as thermal runaway. Despite ongoing research, a comprehensive review and investigation are needed to fully comprehend the precise mechanism and evolutionary process of internal short circuits. The formation and progression of internal short circuits in LIBs are complex and multifaceted, stemming from design flaws, manufacturing defects, or operational conditions that exceed safe parameters, jeopardizing battery longevity and posing safety risks.Various factors contribute to internal short-circuit (ISC), including metallic particle intrusion through the separator, lithium dendrite formation, electrode deformation, or thermal battery abuse. It is essential to comprehend these elements to advance the safety of LIB technologies and guarantee their consistent functionality in EVs. The BMS plays a significant role in EV safety by continuously monitoring [3] and managing the state and essential parameters of the battery pack, such as voltage, current, temperature, and State of Charge (SOC) [4]. However, maintaining appropriate levels of these parameters is vital to avoiding thermal runaway, which can cause excessive heat and damage to the battery [5]. In order to overcome these issues, fault diagnosis is essential to identify and mitigate issues that can meet the safety, performance, and longevity of both the battery and the user [6]. In addition, it also enables early detection of potential issues, including capacity degradation, thermal instability, and internal short circuits, which can pose a risk to the battery's reliability and safety [7]. Advanced impedance-based methods, algorithms analyzing voltage and temperature profiles, sophisticated electrochemical models, and machine learning [8] approaches trained on diverse datasets of battery behaviours are some of the strategies employed to detect internal shorts. Integrating data from multiple sensors enhances detection accuracy through sensor fusion algorithms [9], enabling real-time monitoring and response [10] to short-circuit events. Efforts to standardize performance criteria and testing methods for short-circuit detection algorithms by organizations such as IEEE [11] and SAE [12] are pivotal in ensuring uniformity and reliability across diverse battery systems. These advancements illustrate ongoing efforts to enhance lithium battery safety through advanced detection algorithms as battery technology evolves.

Fig 1 illustrates the key components of a BMS, which plays a crucial role in preventing significant battery malfunctions [13]. Specifically designed for managing Li-ion battery packs with series-parallel connections, the BMS includes a cell monitor responsible for reading the voltages of individual cells [14]. This monitor ensures that the voltage levels across all cells are balanced, a process known as balancing. The

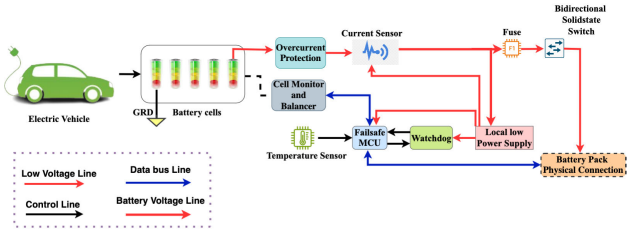

FIGURE 1. Typical structure of battery management system.

balancing function is controlled by a Microcontroller Unit (MCU) embedded within the BMS. The MCU not only oversees the balancing process but also manages telemetry data, switch manipulation, and the overall balancing strategy. This centralized control enables efficient and effective management of the battery pack, enhancing its performance and longevity. In practical applications, there are simplified BMS solutions available for single cells that do not require balancing or MCU functionality. These solutions, as depicted in Fig 2, cater to less complex battery configurations, offering cost-effective alternatives for specific use cases.

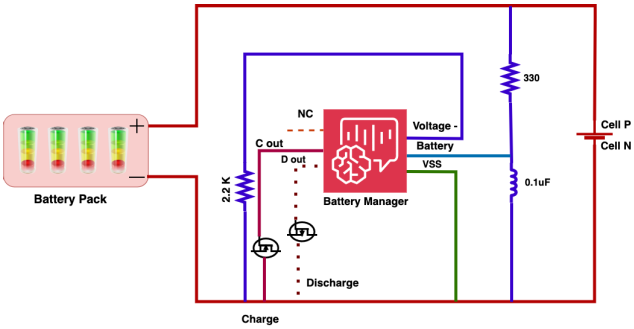

FIGURE 2. Basic structure of battery manager.

The rest of the paper is organized as follows. The Section II presents the recent works related to the topic, while Section III presents the proposed methodology. It is followed by, Section IV which deals with the design of Li-ion battery pack, and Section V describes the background on various anomalies detection algorithms. Further, Section VI details the proposed level shift anomaly detection algorithm, and Section VII evaluates the implementation results. Finally,Section VIII concludes the work and future scope.

II. RELATED WORK AND KEY CONTRIBUTIONS

The detection of short circuit (SC) faults in LIBs is essential due to the potential risks, including rapid battery discharge, which can cause overheating, fires, and even explosions. The fast detection of SC faults protects both the battery and the surrounding environment. Moreover, it can enable accurate maintenance by replacing the affected batteries and minimizing the risk of severe faults in various systems, such as electric vehicles, portable electronic devices, and energy storage systems. As a solution, detection methods are required with the concern of safety, reliability, and long-term

performance of LIBs. For instance, in [15], authors have proposed a model-based fault-diagnosis algorithm for online detection of internal short circuit (ISC) faults in large-format LIBs by considering the Voltage and temperature signals used for robust fault diagnosis. The researchers of [16] and [17] have implemented an Extended Kalman Filter (EKF) algorithm to detect soft ISC faults by extracting the open circuit voltage of the faulted cell, enabling early detection with accurate resistance estimates and onboard soft SC faults for SOC estimation in LIB packs.In addition, in [18] proposed an enhanced EKF algorithm for more precise estimation of the SOC difference and simultaneous quantitative identification of the short circuit resistance magnitude. Further, in [19], authors have proposed a two-step stochastic fault detection and diagnosis algorithm with the concern of identifying faults in LIBs using temperature measurements to enhance reliability in battery performance monitoring. The proposed algorithm has shown better performance than simulations in correcting model errors and identifying faults in LIBs.

In [20], the researchers have proposed a graph-based autoencoder using voltage sensor layout data for fast fault detection in LIB packs, with higher accuracy and quicker detection times than state-of-the-art methods. The researchers of [21] have implemented a real-time data-driven method using improved principal component analysis to diagnose multiple faults in LIBs quickly by enabling fault traceability without complex processes. Moreover, in [22], the authors have presented various fault diagnosis methods, such as K-means for reference cell selection and the Fréchet algorithm for early warning of minor faults in lithium-ion battery packs of real-world electric vehicles. Various researchers have developed a short-circuit fault-diagnosis method for LIBs in energy storage systems using voltage cosine similarity to achieve rapid and effective fault detection based on battery characteristics [23]. In [24] authors have discussed the fault mechanisms, and diagnosis procedures for different faults in LIBs and also discussed the future trends to protect the user and vehicle in a safer condition. The researchers of [25] established a thermal runaway propagation model for 18,650 LIB packs and propose a Mathematical model for combining the thermal runaway electrical and thermal conduction models aiding for safer battery pack design. In [26], the authors have presented a sensor cloud framework integrating heterogeneous wireless sensor networks with a cloud platform. They have introduced an IDS model to select the optimal cluster head based on SNs' energy levels, considering factors like energy, latency, and intra-cluster distance. Additionally, the study has proposed a self-updated CA optimization (SU-COA) and an improved LSTM model for intrusion detection with minimal error using LSTM+ SU-COA compared to higher errors with other methods such as CMBO, PRO, CSO, GWO, and CA. The researchers have proposed a fuzzy-based multi-attributes Un-Equal Clustering approach that demonstrates a 37% improvement in network performance compared to existing algorithms, showcasing its effectiveness in terms of network stability, packet delivery, energy consumption, and network lifetime [27]. Further, the authors have implemented a novel coordinated control approach for hybrid AC/DC microgrids [28]. In addition, they have used model predictive power and voltage control techniques for optimal transfer.

The authors in [29] have proposed a hybrid machine learning framework that includes Convolution Neural Network (CNN) and Gaussian Process Regression (GPR) for joint estimation of SOC and SOH using FBG sensors to capture multi-point strain and temperature. The researchers in [30] reviewed the different methods for estimating the SoC in EV batteries and discussed BMS's significance in hybrid electric vehicles. In this [31], the author reviewed the current research status, technical challenges, and future trends in LIB state estimation models for BMS and outlined the key challenges in BMS and battery state estimation. Furthermore, in [24], authors have proposed Knowledge-based and model-based diagnostic methods for fault mechanisms, features, and diagnosis procedures for various faults in LIBs, emphasizing the importance of advanced fault diagnosis technologies for safe operation. In [32], researchers have proposed neural network models like Multilayer Perceptron (MLP) and Radial Basis Function (RBF) for detecting electric vehicle battery faults, enhancing accuracy through data pre-processing and model testing. The authors in [33] have proposed a fault diagnosis method using an improved RBF neural network for effectively diagnosing LIB pack faults with 100% accuracy by determination of fault levels.

Based on the extensive research conducted by various scholars, it is worth highlighting that the neural network-based approaches have shown better performance in fault detection and diagnosis of LIBs in EVs. Having been motivated by the given literature, this research work proposed to employ anomaly detection techniques using unsupervised machine learning algorithms to detect internal faults in batteries. The following are the contributions of this research:

1) Designing a battery pack system for two-wheeler vehicles under normal and faulty conditions to understand its thermal behaviour in the simulation platform to identify and solve potential thermal issues that may arise during the operation of the battery pack system.
2) Validating the battery pack system's simulated results using a performance real-time target machine and collecting data from a real-time machine under normal and faulty conditions for the accurate evaluation of the battery pack system's performance, which can be used to improve its design and operation.
3) Proposing anomaly detection methods using unsupervised machine learning techniques to identify anomalies from the collected data of normal and faulty conditions to detect potential faults or malfunctions in

the battery pack system, which can be addressed before they cause serious issues.

III. PROPOSED METHODOLOGY

The proposed methodology involves several steps to detect the anomalies in the given temperature data from the performance real time target machine, as shown in Fig. 3. In the first step presents the design of the LIB battery pack system for two-wheeler vehicles during driving under normal and faulty conditions in the MATLAB SIMULINK platform. The second step, which is data acquisition, involves a collection of data on normal and faulty conditions from the performance real-time target machine with the help of a temperature sensor to validate the simulation results of the battery pack. The faulty condition has been created by inserting the short circuit faults in the battery pack using the thermal resistive fault block at different resistive loads by triggering the SC at 0.3sec. The data collection contains various parameters, such as SOC, temperature, current, and voltage. In this work, the temperature data for normal and faulty conditions for various resistive loads, such as 7Ω, 5Ω, 3Ω, and 1Ω have been considered with the concern of reducing the number of fire accidents. To construct the network for our proposed fault detection algorithm, we have carefully selected a specific set of parameters to optimize its performance. The window size is set to 10, defining the sliding window used to segment the data and ensuring the algorithm considers ten consecutive data points at a time for accurate anomaly detection. We specified N-estimators as 100, enhancing robustness and accuracy by using multiple trees to reduce overfitting and improve generalization. Max samples are set at 0.2, meaning each tree in the ensemble is trained on 20% of the total data, promoting diversity among trees and improving detection performance. The contamination parameter, set at 0.2, represents the expected proportion of anomalies in the dataset, fine-tuning the model's sensitivity to detect faults effectively. By setting max features to 1.0, we ensure that all available features are considered, leveraging the full informational content of the data for making split decisions. The random state is set to 42, ensuring the reproducibility of the model by fixing the seed for the random number generator and facilitating consistent results across different runs. Finally, setting verbose to 0 controls the verbosity of the output during the training process, maintaining a clean and uncluttered output, especially when dealing with large datasets or multiple iterations. By carefully selecting these parameters, we have tailored the network to effectively detect anomalies in the data, ensuring accurate and reliable fault detection. Table 1 shows the training parameters. This meticulous parameter tuning is crucial for achieving optimal performance of the proposed algorithm, ultimately contributing to the robustness and efficiency of our fault detection system. The third step involves preparing and preprocessing the data collected, In real-time fault detection, the prompt identification of faults is paramount in mitigating potential damage and upholding system reliability. Data collection has been systematically executed at temperatures below 323 Kelvin(49.85°C) to achieve this objective. The deliberate selection of this specific temperature threshold has been aimed at ensuring ideal conditions for fault detection, thereby fostering a stable environment conducive to accurate and reliable data. The potential influence of external temperature variations on the integrity of measurements was effectively mitigated by conducting data collection within this temperature range. Through the maintenance of controlled temperature parameters, the detection algorithms were able to more effectively discern deviations or anomalies that may serve as indicators of faults. These fault detection algorithms were intricately designed to continuously scrutinize the gathered data, vigilantly monitoring for any indications of irregularities. The ongoing analysis facilitated the expeditious identification of potential faults, thereby enabling swift intervention to rectify any existing issues. The proactive nature of this approach significantly bolstered the system's capacity to respond to faults, thereby reducing the likelihood of prolonged operational disruptions. Real-time identification and mitigation of faults contribute substantially to overall system reliability and safety, preempting minor issues from snowballing into major problems that could precipitate extensive damage and costly downtime. while the final step focuses on developing algorithms that can detect anomalies in the data. The main objective of these algorithms is to ensure early detection and safeguarding of the user and the vehicle.

TABLE 1. Training parameters.

S/No	Hyper parameters	Value
1	Window Size	10
2	N-estimators	100
3	Max Samples	0.2
4	Contamination	0.2
5	Max Features	1.0
6	Random State	42
7	Verbose	0

IV. DESIGN OF LIB PACK MODEL

The model of the LIB pack, which has been developed using MATLAB SIMULINK, is shown in Fig.4. The battery pack is divided into smaller sub-packs, which are then combined in series and parallel. Due to its thermal and electrical stability, the lithium manganese cobalt oxide battery is considered a promising technology for automotive applications. This type of battery provides improved electrical performance due to its lower resistance. The modeled battery pack has a capacity of 62.5 *Ah*, and the cells used are Panasonic - NCR 18650 BF. Additional specifications for the battery cell are listed

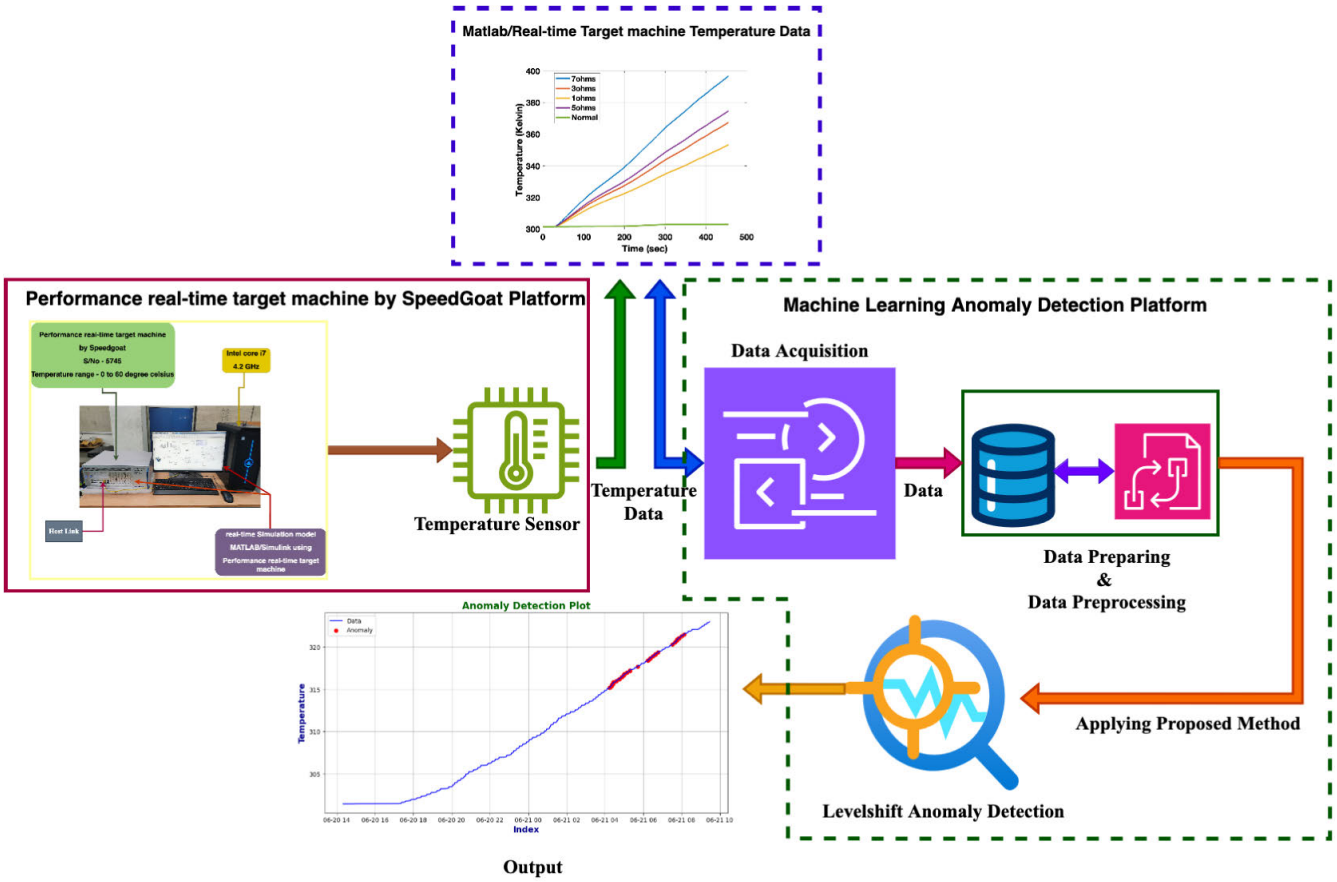

FIGURE 3. Flow chart of proposed methodology.

in Table 2.

$$Number\ of\ cells(series) = \frac{Battery\ pack\ voltage, V}{Cell\ voltage, V} \quad (1)$$

$$Number\ of\ cells(parallel) = \frac{Battery\ pack\ capacity, Ah}{Cell\ capacity, Ah} \quad (2)$$

According to equations 1 and 2 from [34], around 16 cells are connected in series to form a single pack, and 14 of these packs are then connected in parallel to produce a total output of 62.5 *Ah*. In total, the battery pack comprises 224 cells with a weight of approximately 10,528 *grams*. The equivalent discharge model for LIB (Lithium-ion Battery) is depicted in Fig.5. It includes an internal resistance of approximately 0.03-0.05 $m\Omega$, the output rating of the cell charger is $4.2V$ with constant charge of $1.7A$, which results in a voltage drop based on the battery's chemistry. The temperature is an essential factor that affects the LIB's performance in terms of pack voltage, discharge capacity, and power capability. The variation in battery voltage, accounting for temperature effects during discharge, as stated by [35], is expressed by Eq. 3. The assumption is made that the internal resistance (R) changes with the battery's operational temperature,

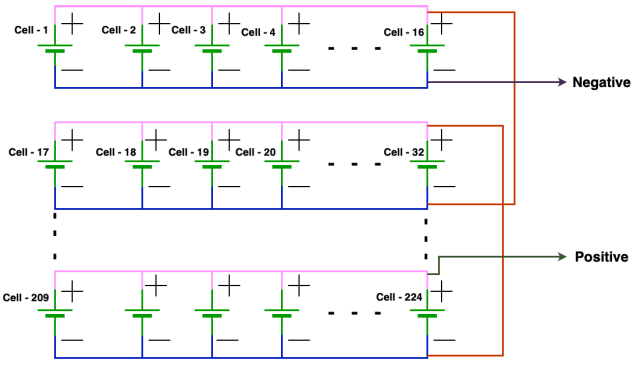

FIGURE 4. Proposed battery pack model in MATLAB simulink.

as stated by [36]. The Arrhenius model included in the discharging Eq. 3 calculates the remaining useful time 'c' in hours, which is acquired through the SIMULINK model for each second.

$$V_batt(xu) = E_0(C) - R(C)\cdot I - K(C)\cdot I \cdot \frac{Q(C_b)}{Q(C_b) - ic} - K \cdot \frac{Q(C_b)}{Q(C_b) - Ic}\cdot Ic + Se^{-D\cdot Ic} \quad (3)$$

TABLE 2. Battery cell specifications.

Parameter	Rating
Nominal Voltage	3.6V
Nominal Capacity	3Ah
Charging Time	6:30hrs
Cell Weight	47 grams
Cell Dimensions	18.6×65.2 mm
Internal Resistance	0.03-0.05 mΩ
Cell Charger	1.7A - 4.2V
Cut-off Voltage	2.5 to 2.75V

where,
$E_0(C)$– constant-voltage,
$K(C)$ – polarisation constant,
$Q(C_b)$– capacity, and
$R(C)$ – internal resistance [36].

FIGURE 5. Schematic representation of Discharge battery model.

V. BACKGROUND

This section presents a comprehensive background of the methods for detecting battery internal faults. Furthermore, it provides a detailed overview of the various models used for identifying faults within the dataset, offering a better understanding of the methodologies utilized in the analysis and diagnosis process. The research discusses the significance of understanding different fault detection algorithms and implementing anomaly detection techniques to identify faults. It stresses the importance of comprehending each algorithm's specifics and mechanisms to understand their strengths and limitations. Implementing anomaly detection involves collecting a comprehensive dataset, training the model, and monitoring real-time data to identify deviations from expected patterns. Anomaly detection methods are highlighted for their general applicability and ease of implementation, making them versatile tools for various applications. The ultimate goal is to establish a reliable and efficient system for real-time fault detection to enhance the overall reliability and safety of the system.

A. MACHINE LEARNING

Using unsupervised algorithms for anomaly detection offers several advantages, particularly in analyzing multiple variables, features, or predictors simultaneously [37]. These approaches allow for detecting anomalies across all variables in the dataset together, as opposed to analyzing each variable separately. Unsupervised anomaly detection methods can be used in two ways, including univariate and multivariate [38]. In univariate anomaly detection, anomalies are identified based on deviations from the normal conditions within a single variable. On the other hand, multivariate anomaly detection considers interactions between variables and detects anomalies based on their collective behaviour, which can provide a more comprehensive understanding of the dataset. By leveraging unsupervised algorithms, analysts can uncover complex relationships and patterns across multiple variables, leading to more accurate anomaly detection [39]. These approaches are essential in datasets where anomalies may be influenced by the interactions between different variables, allowing for a more accurate data analysis.

B. ISOLATION FOREST

The Isolation Forest (IF) algorithm is an unsupervised learning technique used for anomaly detection [40]. This algorithm is designed to identify anomalies in the datasets by learning optimal decision boundaries that isolate these anomalies from instances [41]. Unlike conventional anomaly-based anomaly detection methods, the IF algorithm takes a different approach, which depends on profiling regular data points or calculating distances to identify anomalies. During the training phase, an ensemble of decision trees is created. Splitting points and attributes are randomly selected to construct each tree to divide the data sample. Data analysis continues until a set height, uniform values, or one data point remains in the sample. This random selection process helps prevent overfitting and ensures the trees are not overly focused on local features [42]. The IF algorithm works by separating anomalous data points from normal ones, with consideration of two main assumptions including, anomalies are minor and significant occurrences within the dataset. In the IF algorithm, the isolated trees (iTree) have been initially trained with 100 trees as the default setting, which has been determined to produce optimal results through experimentation, as shown in Fig. 6. Then, it has experimented with increasing the number of trees up to 200 in increments of 20, but no improvement has been detected. As a result, it has been trained with 100 trees to reduce the complexity of the model. During the testing phase of the algorithm, each data point is evaluated by each iTree to determine its anomaly score, represented by s(y). The score ranges from 0 to 1, where values closer to 1 indicate potential anomalies (assigned a value of -1), while those less than 0.5 are classified as normal (assigned a value of 1). Algorithm 1 presents the procedure for detecting temperature variations in the battery pack, as discussed in V-B.

Moreover, the IF algorithm can achieve better computational performance results with data subsampling. Each data

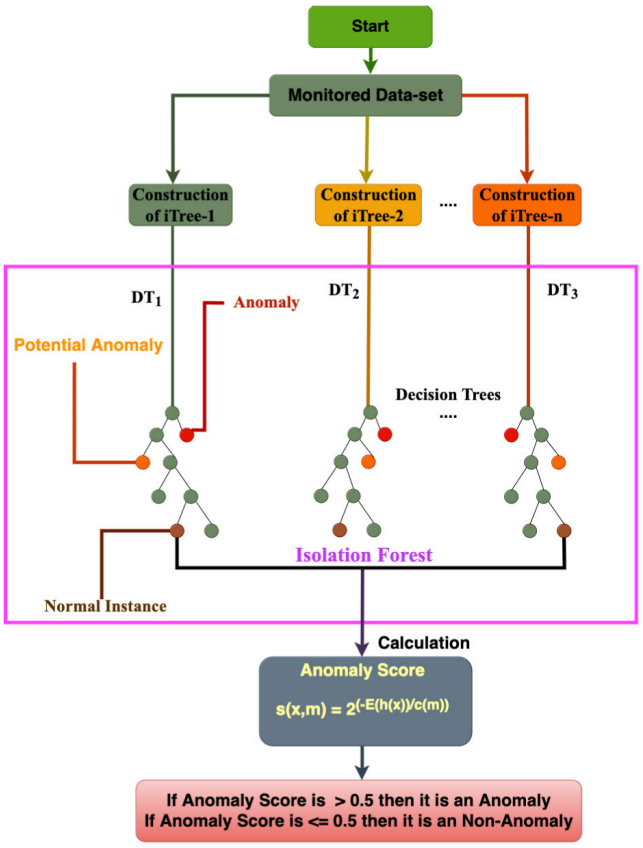

FIGURE 6. Isolation forest classification model architecture.

point in the dataset is assigned a path length, which represents the number of edges traversed from the root node to reach that specific data point in an iTree. The average path length for all data points is calculated as $E(h(y))$ and $c(m)$ is the normalization constant for a dataset of size m. The anomaly score $s(y; m)$ of each data point y is computed to identify anomalies in the dataset. This score depends on the number of samples in the dataset, m. The mathematical representation of the anomaly score is as follows:

$$s(y, m) = 2^{-E(h(y))/c(m)} \tag{4}$$

C. ELLIPTICAL ENVELOP

The Elliptical Envelope (EE) algorithm works by using the centroid of the data as the center of an ellipse as shown in Fig. 7. Each data point's distance from this centroid contributes to forming the elliptical shape, denoted as $'C'$. If a data point's distance from the centroid exceeds this radius, it is classified as an outlier [43]. To determine whether a point is an anomaly, the algorithm uses the inequality where d_1 is the distance of the point from the centroid. If this condition is satisfied, the point is identified as an anomaly. This method effectively identifies anomalies in datasets with a Gaussian distribution, where data points cluster around a mean value. The mathematical representation of the EE algorithm is given

Algorithm 1 Isolation Forest

1: $IsolationForest - X, n_{cif}$
Input: X_{train} - a set of raw faulty data
n_{cif} - contamination rate
Output: Detection of Temperature Variation in the Battery pack
2: $iTrees \leftarrow Forest(X_{train}, n_{cif})$ // Training phase - Learn iTrees
3: $labels \leftarrow (If - predict(x, iTrees)$// predict labels (-1 labels for deviation)
4: **return** Fault data detection

as follows:

$$d_1 > C^2 \tag{5}$$

The algorithm calculates the minimum covariance determinant by finding the covariance matrix in the dataset while excluding the minimum values [42]. This step is important as it helps to identify the most representative covariance among the data points. Points with higher covariance, which indicates a greater deviation from the mean, are considered anomalies. This method is particularly useful in detecting anomalies that deviate significantly from the dataset's normal behavior. Algorithm 2 presents the procedure for detecting temperature variations in the battery pack, as discussed in V-C.

The EE algorithm works in two phases, including learning an elliptic and an anomaly detection phase. The EE algorithm learns an imaginary boundary ellipse during the training phase. Data points within the ellipse, such as inliers, have been labeled with 1, while data points outside the ellipse, such as outliers or anomalies, have been labeled with -1. The algorithm uses the Mahalanobis distance, denoted as D^2, to measure the number of standard deviations between each data point and the mean of the data distribution as shown in Fig. 8. The Mahalanobis distance [44] is calculated for each subsample and each feature dimension. The mathematical representation of the Mahalanobis Distance can be computed as follows:

$$Mahalanobis\ Distance(D)^2 : (y - \mu)^V B^- 1(y - \mu) \tag{6}$$

where, y represents the vector of the data, D^2 represents the Mahalanobis distance, B^-1 represents the inverse covariance matrix of independent variables, μ represents the mean of the subsample distribution, and V represents the vector transpose.

1) EUCLIDEAN DISTANCE

The Euclidean distance formula is commonly used in machine learning to measure the distance between two vectors with real-valued elements. The shortest distance between two points in space is called Euclidean distance and is fundamental in various applications. A visual representation of Euclidean distance is shown in Fig. 9. The Euclidean

Algorithm 2 Elliptical Envelop

$EllipticalEnvelop - X, n_{cEE}$

Input: X_{train} - a set of raw faulty data
n_{cEE} - contamination rate

Output: Detection of Temperature Variation in the Battery pack

2: $elliptical \leftarrow FastMCD(X_{train}, n_{cEE})//Trainingphase-Learnanelliptic$
$labels \leftarrow (EE-predict(x, elliptic)//$ predict labels (-1 labels for deviation)
4: **return** Fault data detection

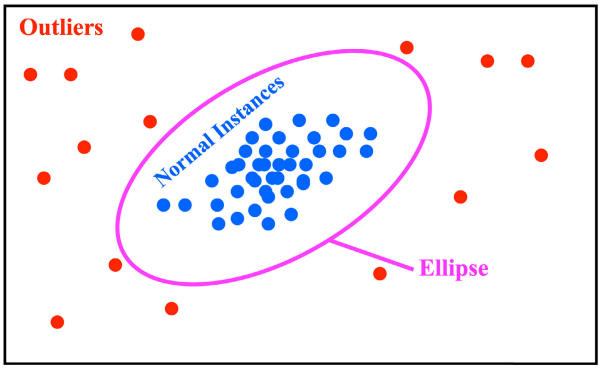

FIGURE 7. Basic elliptical envelop model.

distance can be calculated using the following formula [45]:

$$Euclidean\ Distance : \sqrt{(D_2 - D_1)^2 + (F_2 - F_1)^2} \quad (7)$$

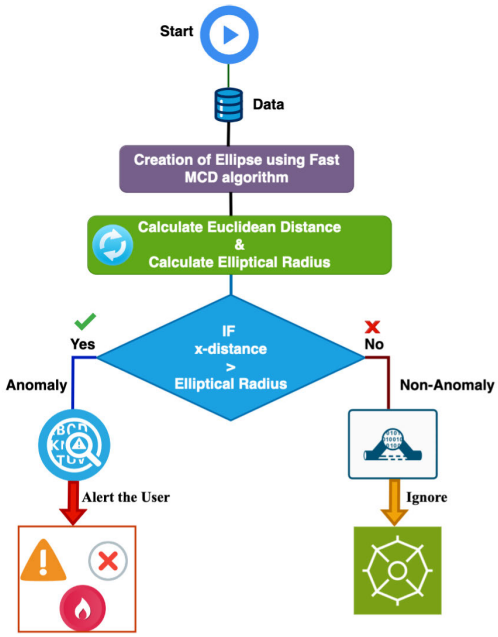

FIGURE 8. Flow of elliptical envelop model.

On the coordinate plane, D_1 and D_2 represent values on the horizontal axis, while F_1 and F_2 represent values on the vertical axis.

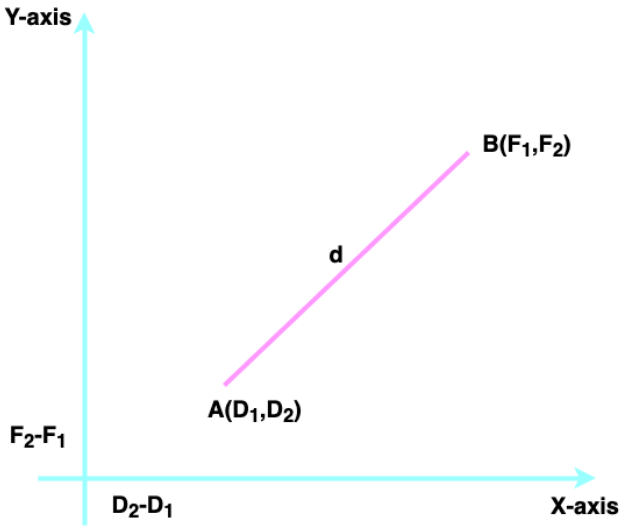

FIGURE 9. Euclidean distance matrix.

VI. PROPOSED LEVEL SHIFT ANOMALY DETECTION

Level shift anomaly detection (LevelShiftAD) is a technique for identifying anomalies in time series data. It works by detecting significant changes or shifts in the overall level of the data. This approach is useful in detecting sudden jumps or drops in the data that may indicate a change in the underlying data generation process. The LevelShiftAD function employs two sliding windows that traverse the data, calculating the statistical measures (median or mean) of the latter and the former windows and computing the difference between them. This difference creates a new time series, denoted as s_1. Next, the function determines the normal range for s_1 using the interquartile range (IQR) approach. It calculates the first quartile (Q_1) and the third quartile (Q_3) of s_1 and then defines the normal range as (Q_1 - c * IQR, Q_1 + c * IQR), where c is a user-defined factor. If the difference between the statistical measures falls outside this normal range, the corresponding point in the original time series is considered an anomaly. Its visual representation is shown in Fig.10.

This approach effectively detects level shift anomalies in time series data without requiring labeled training data. The choice of two essential parameters, window size, and factor c, significantly impacts the performance of the anomaly detection model. The window size specifies the number of data points in each time window. A larger window size makes the model less sensitive to sudden changes in the data, as it considers a longer history of observations. As a result, it can be beneficial in reducing the impact of short-term fluctuations or noise in the data, leading to a more stable detection of anomalies. On the other hand, factor c plays an important role to define the boundaries of the normal range based on the historical IQR. A larger value of c

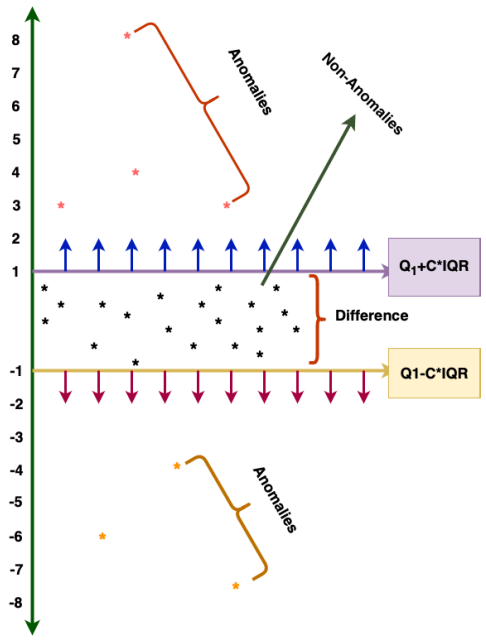

FIGURE 10. Identification of anomalies in LevelshiftAD.

results in a wider normal range, which is suitable for data with higher fluctuations. This wider range accommodates the higher variability in the data, making the model less likely to flag normal fluctuations as anomalies. Conversely, a smaller value of $c$narrows the normal range, making the model more sensitive to deviations from the expected pattern in data with lower fluctuations. The Python package ADTK has been utilized for unsupervised anomaly detection in time series data, specifically for detecting level shift anomalies. Algorithm 3 presents the procedure for detecting temperature variations in the battery pack, as discussed in VI.

Algorithm 3 Proposed Algorithm

$Levelshift - X, n_{cif}$

Input: Define window size: 10
Statistic: Median
Compute Median for the data points in that window for all the data points

3: Calculate the difference between current data point and previous data points(S)
$CalculateQ_1, Q_3, andIQR$
Generate Decision Boundary $(Q_1 + C * IQR(D_1))(Q_1 - C * IQR(D_2))$

Output: Detection of Temperature Variation in the Battery pack

6: labels $\leftarrow$ if $(D_1 <= S_i <= D_2)$// Normal
if $(S_i >= D_1$ and $S_i <= D_2)$// Anomaly//(predict labels (-1 labels for deviation)
return Fault data detection

The proposed methodology comprises several steps to detect anomalies using the levelshiftAD algorithm, as illustrated in Fig. 11. The first step involves collecting raw data from the performance real-time data target machine. The second step involves creating new time-series data using a window size and median. The window size has been selected based on the requirement. In the third step, the *IQR* and quartiles are calculated using the window size. Then, in the fourth step, decision boundaries are calculated using the *IQR* and quartiles. In the final step, it is decided whether the given data points are normal or anomalies using the S_t values.

VII. RESULTS AND DISCUSSIONS

This section presents the results and discussions of the real-time performance of the target machine and the performance of different algorithms in detecting anomalies under various conditions.

A. MECHANISM OF ISC IN LIBS

The ISC in LIBs often plays a significant role in causing mechanical, thermal, and electrical abuses, which can eventually lead to thermal runaway. As a result, there are various factors that can contribute to the development of ISCs in batteries. One of the significant factors is manufacturing imperfections, such as the presence of metal impurities or electrode dislocation [46]. Physical abuse is another contributing factor that causes dropping or crushing the battery [47], [48], [49]. Moreover, improper operation, such as overcharging or exposing the battery to high-temperature environments due to inadequate BMS design, is also a significant cause of ISCs [50], [51], [52]. Figure. 12 provides a detailed overview of the main factors that contribute to ISCs. The following section briefly analyzes the ISC process triggered by several typical incentives.

B. SIMULATION OF BATTERY PACK UNDER ISCS

The simulation environment consists of several interconnected blocks, including thermal resistors, convective heat transfer elements, current sensors, temperature sensors, and voltage sensors. These blocks are connected to simulate faults in the battery system's thermal and electrical network. A simulation environment has been used to design a custom battery pack with a 16P (parallel) 14S (series) connection scheme, which is divided into 7 modules, each consisting of a 16P 2S connection. Each individual cell has specific battery parameters, including a rated voltage of 3.6V, a rated capacity of 3, and a temperature range of 273.15-323.15K. The thermal resistor values have been altered by introducing different resistance values to simulate various faults (e.g., 3, 5, 1, and 7 ohms). Parameters such as convective heat transfer, current sensing, temperature sensing, and voltage sensing have been integrated to conduct these fault simulations. This setup allows for an exhaustive analysis of how various faults impact the battery pack's thermal behavior, providing valuable insights into fault detection. The simulation model includes a thermal resistor block that has a resistance value varying with temperature (T) through a thermal port. The resistance (R) of the thermal resistor at a specific temperature $T$is determined by the following

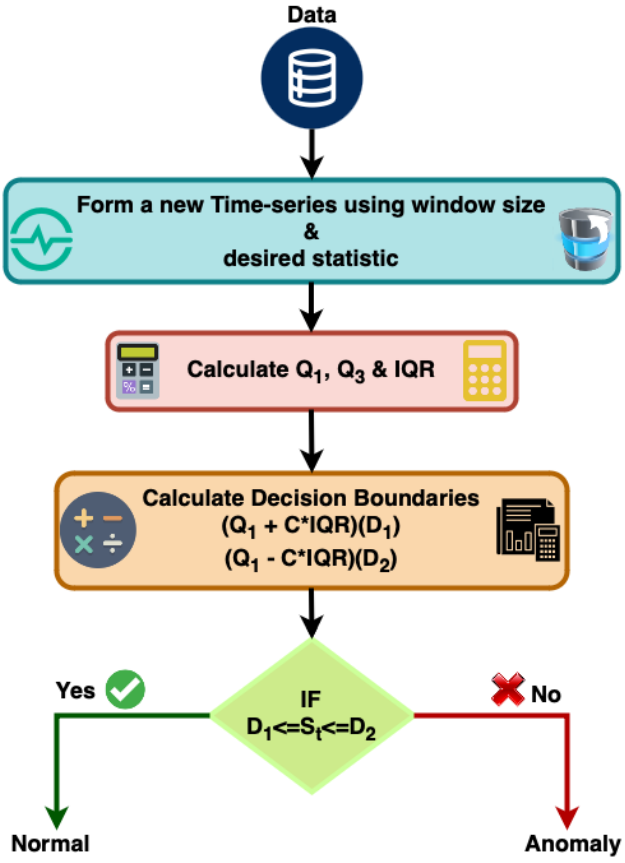

FIGURE 11. Flow chart of levelshiftAD algorithm.

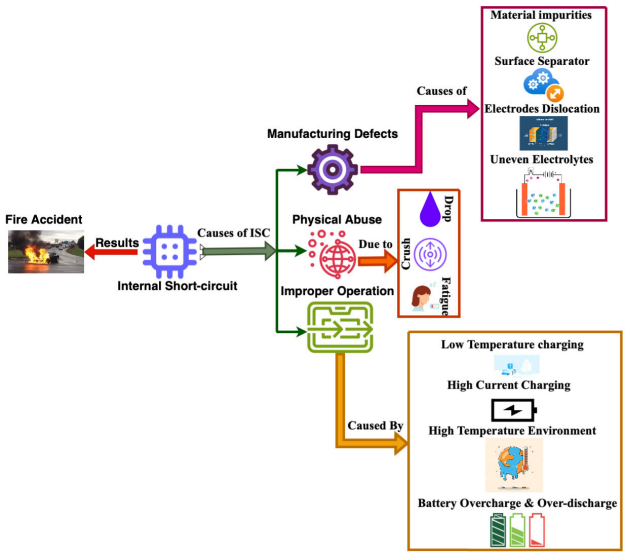

FIGURE 12. Overview of main factors in ISCs.

equation:

$$R(T) = R_0 \times (1 + \alpha(T - T_0)) \tag{8}$$

where:

- RT is the resistance at temperature T,
- R_ref is the reference resistance at reference temperature T_ref,
- α is the temperature coefficient of resistance, and
- T_ref is the reference temperature.

This equation allows the thermal resistor to dynamically adjust its resistance based on the current temperature, providing a more realistic representation of the system's thermal behavior. The convective heat transfer block models heat transfer in thermal networks by accounting for fluid motion convection, which can have varying characteristics. The current sensor block converts electrical current measurements into a proportional physical signal, while the temperature sensor monitors temperature changes within the thermal network. Moreover, the voltage sensor block functions as an efficient voltage sensor, converting voltage measurements into corresponding physical signals. A short circuit within the battery pack significantly impacts important parameters such as current, voltage, temperature, and state of charge. The increase in current leads to a drop in voltage, while the sudden temperature rise results in elevated heat generation, thereby increasing the risk of thermal runaway or fire.

For the simulation, MATLAB version 2023b has been used to design a battery pack under normal and faulty conditions of a two-wheeler vehicle, and outcomes have been validated from MATLAB Simulink using the performance real-time target machine. The target machine's visual representation is shown in Fig. 13. This machine is equipped with an Intel Core i7 processor running at 4.2 GHz, containing 4 cores, and a memory size of 4GB. The machine's Ethernet host link has been used ETH1 (1219 - Index 0), with the MAC address being 00-01-29-9C-AC-0D. Additional specifications for the Real-Time target machine are listed in Table 3. The temperature data has been collected from the battery pack under both normal and faulty conditions using the real-time machine, and the graphical representations of collected temperature data have been demonstrated in Fig.14. Which shows temperature changes caused by thermal resistive faults intentionally introduced into the battery pack. It shows how the temperature rises in the battery pack due to the faults. Moreover, the preparation and preprocessing of the collected temperature data have been carried out, and various algorithms have been used to detect anomalies in the preprocessed data.

Figures 17, 18, and 19 have shown a comprehensive comparison of the performances of the Isolation Forest, Elliptical Envelope, and proposed LevelshiftAD methods. These graphs provide clear insights into the detection capabilities of each method. The Isolation Forest method appears to detect anomalies from various temperature data points but fails to detect faults at the specified threshold limit. Similarly, the Elliptical Envelope method detects faults from temperature data points distant from the threshold limit.

TABLE 3. Real-Time target machine specifications.

Battery	Features
Number of channels	6 (Independent and Isolated)
Output voltage	0.7V (14-bit resolution)
Output voltage accuracy	±0.2%±20mV
Isolation voltage	±750V
Output current source	upto 300mA per channel
Current sink	0 to 100mA (in 16 steps)
Output Connections	Vout+, Vout-
Protection	Short-circuit
Main drive	1TB SSD
Processor	Intel Core i7 4.2 GHz, 4cores
Memory	4 GB
MAC address	00-01-29-9C-AC-0D

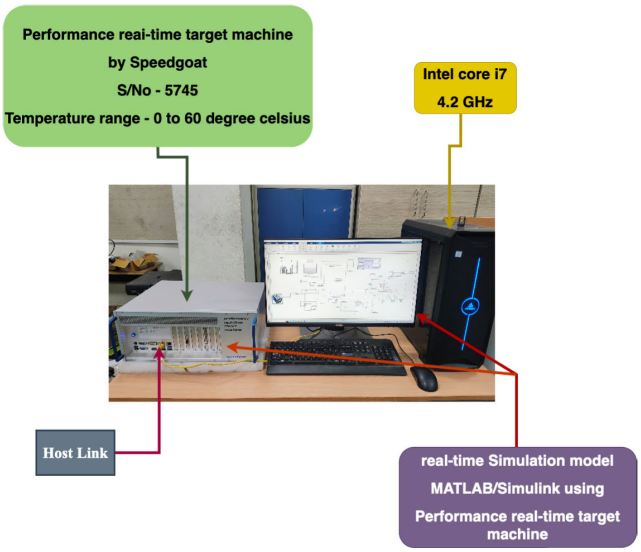

FIGURE 13. Overview of real-time simulation.

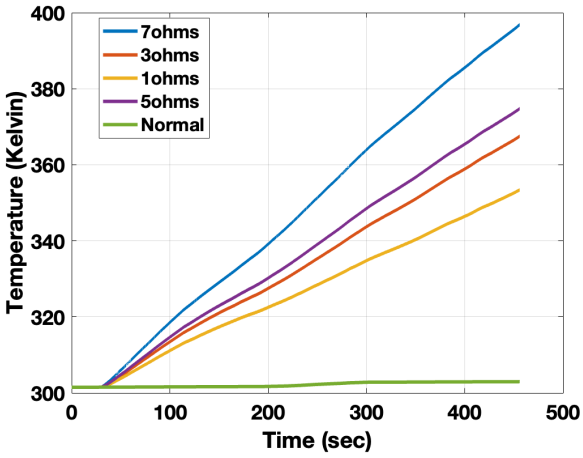

FIGURE 14. Comparison of Temperature Variations.

In contrast, the LevelshiftAD method detects temperature faults accurately at the threshold limit set for the temperature fault. Moreover, It detects faults faster than the other anomaly

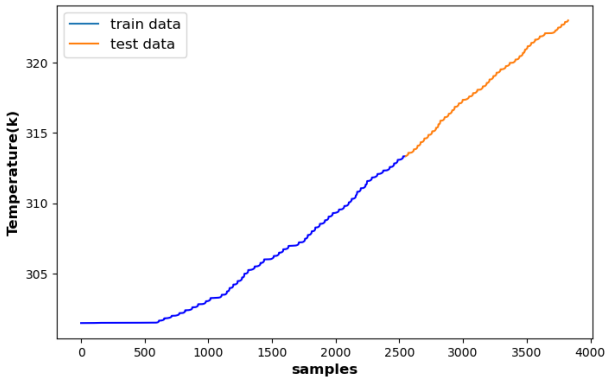

FIGURE 15. Train and test results.

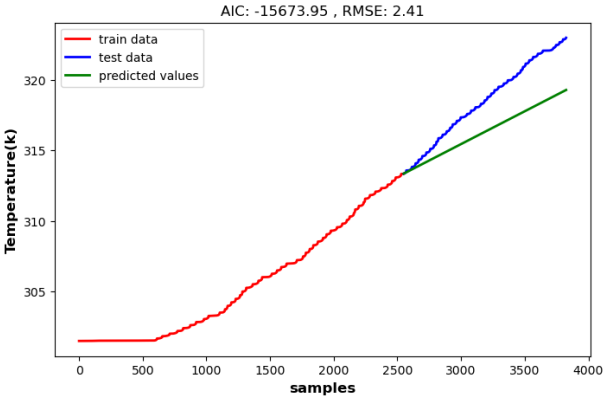

FIGURE 16. Train and test prediction.

detection methods. In this study, the training and testing data is distributed as 2549 and 1,276 in the total dataset with the ratio of 75 - 25% shows in Fig. 15, and then we have trained our algorithm to identify the Root Mean Square Error (RMSE) and Akaike Information Criterion (AIC) to observe the training accuracy.The mathematical representation of the RMSE and AIC training accuracy as follows in equations: 9 and 10

$$RMSE : \sqrt{\frac{1}{m}\sum_{j=1}^{m}(x_j - \hat{x}_j)^2} \tag{9}$$

where: x_j: is the actual value
$\hat{x}_j$: is the predicted value
m: is the number of observations

$$AIC : N * \ln\left(\frac{SS_e}{N}\right) + 2k \tag{10}$$

where: M: denotes number of observations
SS_e: Sum Square of errors
P: is the number of Parameters

Then utilizing the minimum RMSE and AIC score from the training network and we have particularly selected the optimized network to test the model for prediction. Fig. 16 showcases the predicted outcome of the test data.

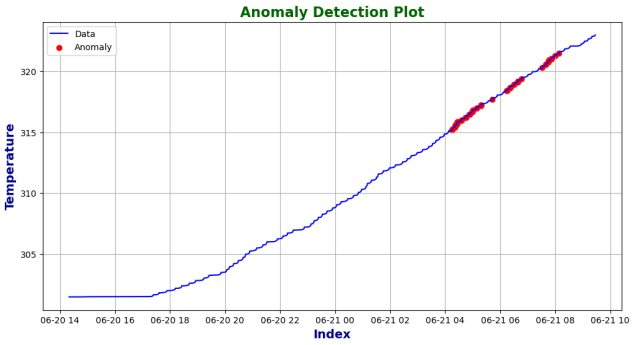

FIGURE 17. Levelshift anomaly detection.

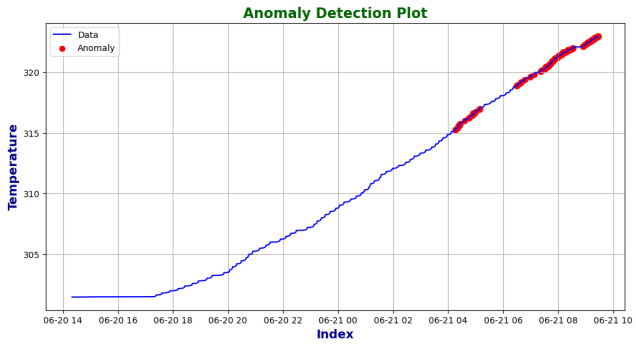

FIGURE 18. Isolation forest anomaly detection.

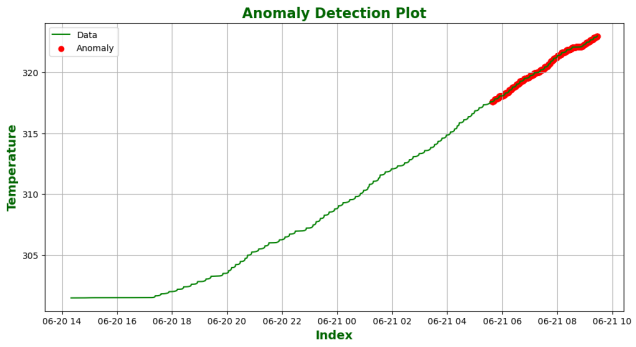

FIGURE 19. Elliptical envelop anomaly detection.

The performance metrics that have been used to evaluate the proposed model. The selected performance metrics comprise Accuracy, Precision, and F1 score, which have been defined according to the [53]. The equations for these metrics are commonly used to evaluate the performance of classification models. The equations for the metrics are represented as follows:

$$Accuracy = \frac{TP + TN}{TP + TN + FP + FN} \tag{11}$$

$$Precision = \frac{TP}{TP + FP} \tag{12}$$

$$F_1 score = 2 * \frac{TP}{2TP + FN + FP} \tag{13}$$

where, $TP, FP, TN, andFN$ stand for True Positive, False Positive, True Negative, and False Negative, respectively. These metrics provide fundamental insights into the accuracy, completeness, and precision of classification models in predicting different classes. This inclusion will ensure that readers understand how the accuracy metric was calculated and can appreciate the context of your results.

VIII. CONCLUSION AND FUTURE WORK

The paper has presented the significance of ISCs in lithium-ion batteries and their potential to cause mechanical, thermal, and electrical abuses that lead to thermal runaway. The literature has identified various factors contributing to the development of ISC, including manufacturing imperfections, physical abuse, and improper operation. As a solution, this paper has presented a simulation environment to analyze the impact of different faults on the battery pack's thermal behaviour, providing valuable insights into fault detection. The simulation model incorporated various blocks such as thermal resistors, convective heat transfer elements, current sensors, temperature sensors, and voltage sensors, allowing for an exhaustive analysis of the system's thermal behaviour. Furthermore, a LevelshiftAD method has been proposed to detect temperature faults accurately at the threshold limit set for the temperature fault, outperforming other anomaly detection methods in terms of accuracy and speed.

For future work, the LevelshiftAD algorithm is suggested to be tested on a physical battery pack in outdoor settings to assess its robustness in different environmental conditions. The study recommends examining additional features beyond position coordinates, such as RGB colors, surface normals, or curvature features, to determine their impact on the proposed solution. Further, the paper suggests exploring how the proposed methodology affects related tasks like segmentation, obstacle detection, and pathfinding for additional insights and research opportunities.

CONFLICT OF INTEREST

We know of no conflicts of interest associated with this publication.

DATA AVAILABILITY STATEMENT

Data will be available based on the reasonable request to the corresponding author [A. Rammohan].

ACKNOWLEDGMENT

The authors would like to thank Vellore Institute of Technology (VIT) for providing licensed tools for this research.

REFERENCES

[1] M. A. Hannan, M. S. H. Lipu, A. Hussain, and A. Mohamed, "A review of lithium-ion battery state of charge estimation and management system in electric vehicle applications: Challenges and recommendations," *Renew. Sustain. Energy Rev.*, vol. 78, pp. 834–854, Oct. 2017.

[2] M. H. Abd Wahab, N. I. M. Anuar, R. Ambar, A. Baharum, S. Shanta, M. S. Sulaiman, and H. Hanafi, "IoT-based battery monitoring system for electric vehicle," *Int. J. Eng. Technol.*, vol. 7, no. 4, pp. 505–510, 2018.

[3] E. S. Altuntop, D. Erdemir, Y. Kaplan, and V. Özceyhan, "A comprehensive review on battery thermal management system for better guidance and operation," *Energy Storage*, vol. 5, no. 8, p. e501, Dec. 2023.

[4] H.-F. Ji and Z. H. Shaik, "Protecting conductive polymer wire from oxidation using an air-impermeable polyisobutylene coating," *Thin Solid Films*, vol. 488, nos. 1–2, pp. 149–152, Sep. 2005.

[5] M. Shen and Q. Gao, "A review on battery management system from the modeling efforts to its multiapplication and integration," *Int. J. Energy Res.*, vol. 43, no. 10, pp. 5042–5075, Aug. 2019.

[6] B. Balasingam, M. Ahmed, and K. Pattipati, "Battery management systems—Challenges and some solutions," *Energies*, vol. 13, no. 11, p. 2825, Jun. 2020.

[7] M. Brandl, H. Gall, M. Wenger, V. Lorentz, M. Giegerich, F. Baronti, G. Fantechi, L. Fanucci, R. Roncella, R. Saletti, S. Saponara, A. Thaler, M. Cifrain, and W. Prochazka, "Batteries and battery management systems for electric vehicles," in *Proc. Design, Autom. Test Eur. Conf. Exhib. (DATE)*, Mar. 2012, pp. 971–976.

[8] Z. Guo, X. Qiu, G. Hou, B. Y. Liaw, and C. Zhang, "State of health estimation for lithium ion batteries based on charging curves," *J. Power Sources*, vol. 249, pp. 457–462, Mar. 2014.

[9] C. Hu, B. D. Youn, and J. Chung, "A multiscale framework with extended Kalman filter for lithium-ion battery SOC and capacity estimation," *Appl. Energy*, vol. 92, pp. 694–704, Apr. 2012.

[10] C. R. Birkl, M. R. Roberts, E. McTurk, P. G. Bruce, and D. A. Howey, "Degradation diagnostics for lithium ion cells," *J. Power Sources*, vol. 341, pp. 373–386, Feb. 2017.

[11] Y. Ye, C. Chen, J. Jin, and L. He, "Li-ion battery management chip for multi-cell battery pack," in *Proc. APCCAS - IEEE Asia–Pacific Conf. Circuits Syst.*, Nov. 2008, pp. 534–537.

[12] *Electric and Hybrid Electric Vehicle Rechargeable Energy Storage System (RESS) Safety and Abuse Testing*, Battery Saf. Standards Committee, SAE Int., Warrendale, PA, USA, 2021.

[13] D. Andrea, *Battery Management Systems for Large Lithium-Ion Battery Packs*. Norwood, MA, USA: Artech House, 2010.

[14] R. Korthauer, *Lithium-Ion Batteries: Basics and Applications*. Cham, Switzerland: Springer, 2018.

[15] X. Feng, Y. Pan, X. He, L. Wang, and M. Ouyang, "Detecting the internal short circuit in large-format lithium-ion battery using model-based fault-diagnosis algorithm," *J. Energy Storage*, vol. 18, pp. 26–39, Aug. 2018.

[16] M. Seo, T. Goh, M. Park, and S. W. Kim, "Detection method for soft internal short circuit in lithium-ion battery pack by extracting open circuit voltage of faulted cell," *Energies*, vol. 11, no. 7, p. 1669, Jun. 2018.

[17] R. Yang, R. Xiong, and W. Shen, "On-board diagnosis of soft short circuit fault in lithium-ion battery packs for electric vehicles using an extended Kalman filter," *CSEE J. Power Energy Syst.*, vol. 8, no. 1, pp. 258–270, Jan. 2022.

[18] L. Yi, X. Cai, Y. Wang, B. Luo, J. Liu, and B. Liu, "Soft short-circuit fault diagnosis of the lithium-ion battery pack based on an improved EKF algorithm," *Recent Patents Mech. Eng.*, vol. 16, no. 2, pp. 138–149, Apr. 2023.

[19] J. Son and Y. Du, "Model-based stochastic fault detection and diagnosis of lithium-ion batteries," *Processes*, vol. 7, no. 1, p. 38, Jan. 2019.

[20] G. Ma, S. Xu, and C. Cheng, "Fault detection of lithium-ion battery packs with a graph-based method," *J. Energy Storage*, vol. 43, Nov. 2021, Art. no. 103209.

[21] X. Gu, Y. Shang, C. Li, Y. Zhu, B. Duan, J. Li, and W. Zhao, "An early multi-fault diagnosis method of lithium-ion battery based on data-driven," in *Proc. 41st Chin. Control Conf. (CCC)*, Jul. 2022, pp. 5206–5210.

[22] M. Wu, W. Du, F. Zhang, N. Zhao, J. Wang, L. Wang, and W. Huang, "Fault diagnosis method for lithium-ion battery packs in real-world electric vehicles based on K-means and the Fréchet algorithm," *ACS Omega*, vol. 7, no. 44, pp. 40145–40162, Nov. 2022.

[23] X. Wu, Z. Wei, T. Wen, J. Du, J. Sun, and A. A. Shtang, "Research on short-circuit fault-diagnosis strategy of lithium-ion battery in an energy-storage system based on voltage cosine similarity," *J. Energy Storage*, vol. 71, Nov. 2023, Art. no. 108012.

[24] X. Hu, K. Zhang, K. Liu, X. Lin, S. Dey, and S. Onori, "Advanced fault diagnosis for lithium-ion battery systems: A review of fault mechanisms, fault features, and diagnosis procedures," *IEEE Ind. Electron. Mag.*, vol. 14, no. 3, pp. 65–91, Sep. 2020.

[25] Y. Jia, M. Uddin, Y. Li, and J. Xu, "Thermal runaway propagation behavior within 18,650 lithium-ion battery packs: A modeling study," *J. Energy Storage*, vol. 31, Oct. 2020, Art. no. 101668.

[26] R. B. Kagade and N. Vijayaraj, "Intrusion detection via optimal tuned LSTM model with trust and risk level evaluation," *Int. J. Bio-Inspired Comput.*, vol. 23, no. 1, pp. 39–52, 2024.

[27] A. Srivastava and P. K. Mishra, "Fuzzy based multi-criteria based cluster head selection for enhancing network lifetime and efficient energy consumption," *Concurrency Comput., Pract. Exper.*, vol. 36, no. 4, p. e7921, Feb. 2024.

[28] S. Shobana and B. K. Gnanavel, "Optimised coordinated control of hybrid AC/DC microgrids along PV-wind-battery: A hybrid based model," *Int. J. Bio-Inspired Comput.*, vol. 20, no. 3, pp. 193–208, 2022.

[29] Y. Li, K. Li, X. Liu, X. Li, L. Zhang, B. Rente, T. Sun, and K. T. V. Grattan, "A hybrid machine learning framework for joint SOC and SOH estimation of lithium-ion batteries assisted with fiber sensor measurements," *Appl. Energy*, vol. 325, Nov. 2022, Art. no. 119787.

[30] H. Rahimi-Eichi, U. Ojha, F. Baronti, and M.-Y. Chow, "Battery management system: An overview of its application in the smart grid and electric vehicles," *IEEE Ind. Electron. Mag.*, vol. 7, no. 2, pp. 4–16, Jun. 2013.

[31] L. Zhou, X. Lai, B. Li, Y. Yao, M. Yuan, J. Weng, and Y. Zheng, "State estimation models of lithium-ion batteries for battery management system: Status, challenges, and future trends," *Batteries*, vol. 9, no. 2, p. 131, Feb. 2023.

[32] S. Shete, P. Jog, R. Kamalakannan, J. T. A. Raghesh, S. Manikandan, and R. K. Kumawat, "Fault diagnosis of electric vehicle's battery by deploying neural network," in *Proc. 6th Int. Conf. I-SMAC (IoT Social, Mobile, Anal. Cloud) (I-SMAC)*, Nov. 2022, pp. 346–351.

[33] J. Wang, S. Zhang, and X. Hu, "A fault diagnosis method for lithium-ion battery packs using improved RBF neural network," *Frontiers Energy Res.*, vol. 9, Aug. 2021, Art. no. 702139.

[34] I. Buchmann, *Batteries in a Portable World: A Handbook on Rechargeable Batteries for Non-Engineers*. Canada: Cadex Electronics Inc, 2001.

[35] A. Rammohan, Y. Wang, S. Kannappan, S. Kumar, B. Ashok, H. Kotb, K. M. AboRas, and A. Yousef, "Service life estimation of electric vehicle lithium-ion battery pack using Arrhenius mathematical model," *Frontiers Energy Res.*, vol. 12, Apr. 2024, Art. no. 1359596.

[36] Z. An, Y. Zhao, X. Du, T. Shi, and D. Zhang, "Experimental research on thermal-electrical behavior and mechanism during external short circuit for $LiFePO_4$ Li-ion battery," *Appl. Energy*, vol. 332, Feb. 2023, Art. no. 120519.

[37] X. Gu, Y. Shang, Y. Kang, J. Li, Z. Mao, and C. Zhang, "An early minor-fault diagnosis method for lithium-ion battery packs based on unsupervised learning," *IEEE/CAA J. Autom. Sinica*, vol. 10, no. 3, pp. 810–812, Mar. 2023.

[38] P. Kumar and A. S. Hati, "Review on machine learning algorithm based fault detection in induction motors," *Arch. Comput. Methods Eng.*, vol. 28, no. 3, pp. 1929–1940, May 2021.

[39] J. Zhang, Y. Wang, B. Jiang, H. He, S. Huang, C. Wang, Y. Zhang, X. Han, D. Guo, G. He, and M. Ouyang, "Realistic fault detection of Li-ion battery via dynamical deep learning," *Nature Commun.*, vol. 14, no. 1, p. 5940, Sep. 2023.

[40] F. T. Liu, K. M. Ting, and Z.-H. Zhou, "Isolation forest," in *Proc. 8th IEEE Int. Conf. Data Mining*, Feb. 2009, pp. 413–422.

[41] J. Jiang, T. Li, C. Chang, C. Yang, and L. Liao, "Fault diagnosis method for lithium-ion batteries in electric vehicles based on isolated forest algorithm," *J. Energy Storage*, vol. 50, Jun. 2022, Art. no. 104177.

[42] Y. Regaya, F. Fadli, and A. Amira, "Point-denoise: Unsupervised outlier detection for 3D point clouds enhancement," *Multimedia Tools Appl.*, vol. 80, no. 18, pp. 28161–28177, Jul. 2021.

[43] B. Hoyle, M. M. Rau, K. Paech, C. Bonnett, S. Seitz, and J. Weller, "Anomaly detection for machine learning redshifts applied to SDSS galaxies," *Monthly Notices Roy. Astronomical Soc.*, vol. 452, no. 4, pp. 4183–4194, Aug. 2015.

[44] W. J. Lee, G. P. Mendis, M. J. Triebe, and J. W. Sutherland, "Monitoring of a machining process using kernel principal component analysis and kernel density estimation," *J. Intell. Manuf.*, vol. 31, no. 5, pp. 1175–1189, Jun. 2020.

[45] Y. S. Park and Y.-S. Lee, "Diagnostic cluster analysis of mathematics skills," *IERI Monograph Ser., Issues Methodologies Large-Scale Assessments*, vol. 4, pp. 75–107, Jan. 2011.

[46] X. Lai, C. Jin, W. Yi, X. Han, X. Feng, Y. Zheng, and M. Ouyang, "Mechanism, modeling, detection, and prevention of the internal short circuit in lithium-ion batteries: Recent advances and perspectives," *Energy Storage Mater.*, vol. 35, pp. 470–499, Mar. 2021.

[47] L. Liu, X. Feng, M. Zhang, L. Lu, X. Han, X. He, and M. Ouyang, "Comparative study on substitute triggering approaches for internal short circuit in lithium-ion batteries," *Appl. Energy*, vol. 259, Feb. 2020, Art. no. 114143.
[48] X. Zhang, E. Sahraei, and K. Wang, "Li-ion battery separators, mechanical integrity and failure mechanisms leading to soft and hard internal shorts," *Sci. Rep.*, vol. 6, no. 1, p. 32578, Sep. 2016.
[49] W. Hao, J. Xie, and F. Wang, "The indentation analysis triggering internal short circuit of lithium-ion pouch battery based on shape function theory," *Int. J. Energy Res.*, vol. 42, no. 11, pp. 3696–3703, Sep. 2018.
[50] H. Wang, E. Lara-Curzio, E. T. Rule, and C. S. Winchester, "Mechanical abuse simulation and thermal runaway risks of large-format Li-ion batteries," *J. Power Sources*, vol. 342, pp. 913–920, Feb. 2017.
[51] C. Wang, Y. Zhu, F. Gao, C. Qi, P. Zhao, Q. Meng, J. Wang, and Q. Wu, "Thermal runaway behavior and features of $LiFePO_4$ /graphite aged batteries under overcharge," *Int. J. Energy Res.*, vol. 44, no. 7, pp. 5477–5487, Jun. 2020.
[52] F. Larsson and B.-E. Mellander, "Abuse by external heating, overcharge and short circuiting of commercial lithium-ion battery cells," *J. Electrochem. Soc.*, vol. 161, no. 10, pp. A1611–A1617, 2014.
[53] Y. Xu, X. Ge, and W. Shen, "A novel set-valued sensor fault diagnosis method for lithium-ion battery packs in electric vehicles," *IEEE Trans. Veh. Technol.*, vol. 72, no. 7, pp. 8661–8671, Mar. 2023.

DASARI HETHU AVINASH received the B.Tech. degree in electrical and electronics engineering from Anna University, Chennai, in 2017, and the M.Tech. degree in renewable energy resources from Karunya University, Coimbatore, in 2020. He is currently pursuing the Ph.D. degree with the School of Electrical Engineering, Vellore Institute of Technology University (VIT), Vellore. His research interests include solar Pv modules, faults in solar panels, electrical vehicles, lithium-ion battery fault detection and isolation, battery management system (BMS), hardware in loop (HIL), and artificial intelligence (AI).

A. RAMMOHAN received the master's degree in embedded systems from SASTRA in collaboration with NTU, Singapore, and the Ph.D. degree in automotive electronics from Vellore Institute of Technology (VIT), Vellore, India. He is currently a Faculty Member with the Automotive Research Centre (ARC), VIT. Before VIT, he was an Research and Development Engineer with NCR Corporation, Scotland. He has a decade of teaching and research experience in the field of predictive algorithms, thermal imaging applications, electronics cooling, and battery management systems in both India and abroad. He has published Thompson and Scopus-indexed articles in reputed journals. He has filed eight patents in the field of automotive electronics out of which two patents have been granted by Indian Patent Office. He has trained more than 1300 students through 41 workshops, 16 certificate courses, and corporate training in the fields of EV battery management systems, automotive electronics, embedded systems, and the IoT.